



full-body posture goals were computed in [12] by utilizing Rapidly-exploring Random Trees. Unfortunately, the planner can only handle a fixed position for either one or both feet, and hence it is difficult to be applied directly in obstacle stepping-over.

Tasks involving object manipulation through contact have mainly been investigated for pushing [8], [5], [15] and lifting [6]. However, there have not been so many research studies on the implementation of dextrous tasks using a humanoid robot. This is due to the difficulty in manipulating an object by two hands while keeping body balance at the same time. We introduce, therefore, a pivoting manipulation of an object that has advantages in terms of precise and stable manipulation compared to the above methods.

### III. PLANNING METHOD OF STEPPING OVER

#### A. Brief Review of Feasibility

Before plan motion for a humanoid robots to step over an obstacle, it must be known whether the robot can do so. We have proposed a method for this feasibility analysis [4], on which our motion planning is based.

In the analysis, we took rectangular objects as typical obstacles, and considered the geometry of the obstacle (height and depth), the sizes, shapes and kinematics of the robot legs. For a given obstacle depth (width in 2-D case), there must be a maximum height of the obstacle that the robot can step over. So we found this maximum height using optimal technique. If the height of an obstacle is less than the maximum one, then the robot can step over the obstacle. Thus we cast the problem into optimization models, where the objective functions are the obstacle heights to be maximized, the variables include the height itself, the distance between the obstacle and the feet, and joint angles of the legs. The constraints include those on collision avoidance, robot balance and joint angles. Motivated by computational geometry, collision-free constraints are formulated using signed areas of triangles, since they can completely describe the geometric relationship between three ordered points or one point and one directed line segment, e.g., one point is to the left or right of a directed line. Based on this, after described the obstacle and the robot legs by their topological features (vertices as points and edges as line segments), we formulated easily the collision avoidance for two line segments. For robot balance, we took the center of mass (CoM) in quasi-static state as a criterion, which is a function of all joint angles of the robot. If the projection of the CoM on the ground is within the supporting area(s), then the robot can keep balance.

For one robot, we may make a series of calculation for the maximum heights of obstacles with different depths, and then make a database mapping the depth and the maximum height of the obstacle, the step-length, and the waist position, respectively, for online and real-time application.

#### B. Planning of Trajectories

In obstacle stepping-over, the procedure is similar to a normal walking. It consists of three phases. In the planning, we consider them separately. Specifically, in phase 1

(single-support), phase 2 (double-support) and phase 3 (single-support), we plan the trajectories of the lifted front foot, the waist trajectory, and the withdrawn rear foot, respectively.

The algorithm can be depicted by the block diagram shown in Fig. 1. The step length and the robot position with respect to the obstacle are first determined according to the obstacle size based on our previous results of feasibility [4]. The step length  $s_l$  of the legs can be set as  $s_l = (s_{vo1} + s_{vo2}) / 2$ , where  $s_{vo1}$  and  $s_{vo2}$  are the two feasible step lengths for the robot to step over two “virtual obstacles” VO1 and VO2, respectively, (Fig. 2a). VO1 is the virtual obstacle with the same depth  $w$  as the real obstacle and with the maximum height  $h_{max}$  corresponding to  $w$ , found in feasibility analysis; and VO2 is the one with the same height  $h$  as the real obstacle and with the maximum depth corresponding to  $h$ , also found in

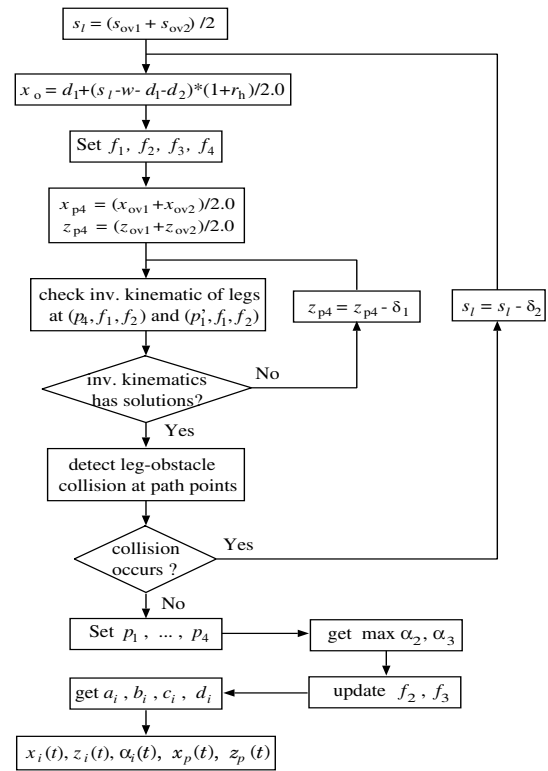
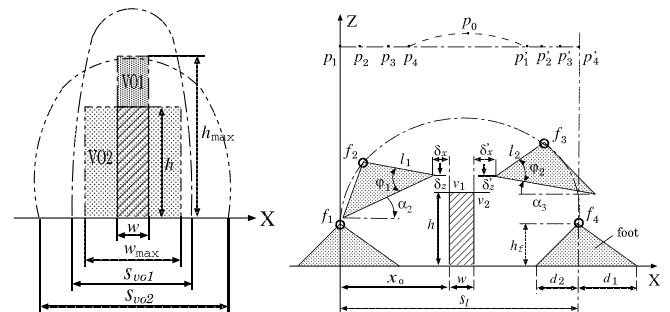


Fig. 1. The algorithm for trajectory planning



(a) Virtual parameters

(b) Foot trajectory

Fig. 2. Parameters for foot trajectories

feasibility analysis.  $s_{vo1}$  and  $s_{vo2}$  can be obtained by looking up and interpolating the feasibility mapping. The setting of step length in this way is adaptive to various obstacles that the robot can step over.

After the step length is determined, the distance between the robot and the obstacle  $x_o$  is set according to the obstacle depth  $w$ , step length  $s_l$  and foot size  $d_1$  and  $d_2$ :

$$x_o = d_1 + (s_l - w - d_1 - d_2)(1 + h/h_{max})/2 \Delta. \quad (1)$$

Foot trajectories are determined by four path control points, where the distance between the end-points  $f_1$  and  $f_4$  is the step length, as shown in Fig. 2b. The two interior points  $f_2$  and  $f_3$  are set with the consideration of collision avoidance, according to the gaps  $x', z'$  and  $x'', z''$ , between the feet and the obstacle, and the feasible orientation angles  $\alpha_2$  and  $\alpha_3$  of the feet, which can be estimated by the inverse kinematics of the legs according to the positions of the waist and the foot. The foot trajectories are in sagittal planes, and each of their components is interpolated using two forth-order polynomials and one third-order polynomial:

$$\begin{cases} F_1(t) = a_1 + b_1 t + c_1 t^2 + d_1 t^3 + e_1 t^4 \\ F_2(t) = a_2 + b_2 t + c_2 t^2 + d_2 t^3 \\ F_3(t) = a_3 + b_3 t + c_3 t^2 + d_3 t^3 + e_3 t^4 \end{cases} \quad (2)$$

where  $F_i(t)$  may be  $x_i(t), z_i(t)$  or  $\alpha_i(t)$ , the X and Z coordinates of path points or the corresponding sole orientation. The coefficients  $a_i, b_i, c_i, d_i$  and  $e_i$  for the polynomials can be easily and uniquely obtained by the following boundary conditions: (a) the curve is continuous at the interior control points, (b) it is also smooth at these points, i.e., the first derivatives of adjacent segments at these points are equal, (c) the second derivatives also match at the interior control points, and (d) the first derivatives at end-points be zero, (e) the second derivatives at end-points be also zero. Under these conditions, the curve would be very smooth [2].

The waist trajectory can also be interpolated in a similar way using polynomials. For simplicity, the height of the waist can be kept constant during the whole procedure. The displacement in X direction and the height of the waist in phase 1 can be set according to the two ‘‘virtual obstacles’’ as follows:

$$x_{p4} = (x_{vo1} + x_{vo2})/2 \Delta, \quad z_{p4} = (z_{vo1} + z_{vo2})/2 \Delta. \quad (3)$$

where  $x_{vo1}$  and  $x_{vo2}$  are the X-coordinates of the waist corresponding to the stepping-over the two ‘‘virtual obstacles’’ VO1 and VO2;  $z_{vo1}$  and  $z_{vo2}$  are the Z-coordinates of the waist. They are obtained in the feasibility analysis. In phase 2, considering avoidance of collision between the leg and the obstacle, the waist height may be increased in the middle when necessary. For lateral motion of the waist, we give the middle point as the interior path control point. Thus the components of the trajectory can be controlled by three points and then interpolated using two fourth-order polynomials, respectively.

After the trajectories have been generated, the motion of the leg joints can be easily obtained by the kinematics of the legs.

### C. Upper-body Motion and Balance Maintenance

Humanoid robots are redundant systems for most motion. This redundancy can be used for various tasks or targets. While the motion of lower body is planned for overcoming the obstacles without any collision, the motion of the lower body is generated with consideration of robot balance, based on RMC [9].

It is well known that, for a humanoid robot to walk stably, the ZMP (Zero Moment Point) must be within the convex hull of the supporting area(s). As stated previously, in our planning, though the lower body of the robot is controlled to realize the desired trajectories under the constraints of collision avoidance, the upper body (including the chest, the head and the two arms) is free and can be used to adjust the ZMP or CoM to keep the robot balance. Currently we control the CoM of the robot so that it is always within the convex hull of the supporting area(s) to maintain robot balance. Since the linear momentum  $P$  depends on the time derivative of CoM position  $r$  through the total mass  $m$  as  $P = m \dot{r}$ , the position of CoM can be controlled by manipulating the linear momentum as  $P = k m (\tilde{r} - r)$ , where the tilde denotes the reference value, and  $k$  is the gain of the control scheme. Using this equation we can calculate the desired linear momentum  $P$  to control the robot CoM. In our system, these values are controlled automatically during the stepping-over.

## IV. PIVOTING MANIPULATION TASK

We describe briefly the pivoting task implemented in this section. We take a simple example of task to manipulate a cuboid object on a plane. We assume that the shape and the physical parameters of the object are known and that the robot grasps the object by two hands firmly without slipping at the contact points.

The manipulation is executed by repeating the following two phases (Fig. 3):

- **Manipulation phase:** The manipulation is done in a quasi-static way by repeating rotation of the object about an axis. Internal force to grasp the object is controlled using impedance control.
- **Robot motion phase:** The robot moves towards the object with the hands at the same position to continue manipulation. The body motion is planned through RMC.

### A. Manipulation phase

The pivoting is performed by repeating the following sequences (Fig. 3).

- 1) The object is inclined by angle  $\theta$  around an axis  $a$  so that it contacts the plane at vertex  $v$  (Fig. 4a).
- 2) The object is rotated by angle  $\phi$  around the vertical axis  $z$  on vertex  $v$  to move to the desired direction (Fig. 4b).
- 3) The object is rotated by  $\psi$  around the rotated axis  $a'$  until the bottom edge touches ground. (Fig. 4c).
  - a) If the object displacement exceeds a value  $D$ , the robot steps toward the desired direction.
  - b) Otherwise back to step 1 or the end of the motion.

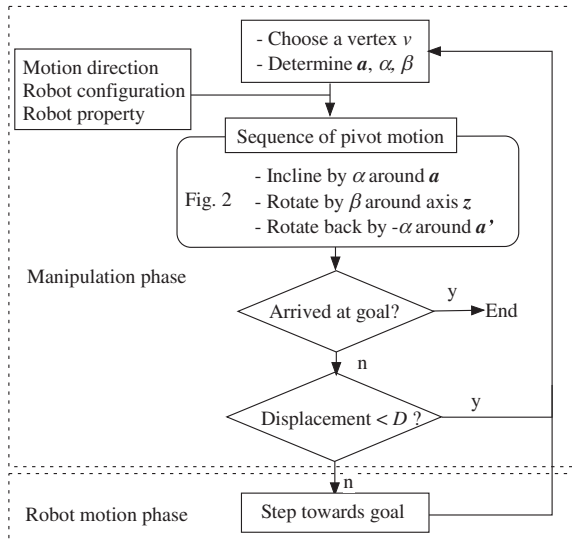


Fig. 3. Flow of pivoting manipulation

The parameters  $\alpha$ ,  $\beta$ , and  $D$  must be designed so that the manipulated object follows the desired trajectory (Fig. 5). The working area and physical properties of the robot body must also be taken into account.

The  $a$  axis and the vertex around which to incline the object are selected not to lose the stability of the robot and the object. The axis  $z$  is set to the vertical axis since no work is required for quasi-static motion around this axis. The angle  $\alpha$  depends on the constraint of robot motion capability as well as the desired trajectory of the robot. To execute more complicated trajectory than that of Fig. 5, we will need a strategy how to determine those parameters, taking account of combination of stepping motion.

Since we assume quasi-static motion, we adopt position control for robot hands to achieve the trajectory for the desired motion. For position-controlled robot as HRP-2, the output of the following impedance control is added to the position

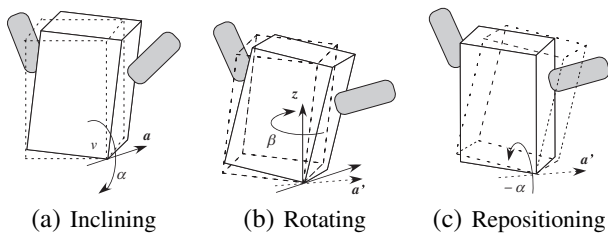


Fig. 4. Sequence of pivot motion of cuboid

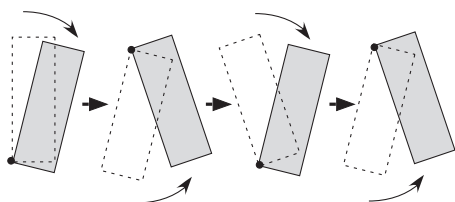


Fig. 5. Object transporting by repeated pivoting (top view)

command of manipulation to regulate the internal force.

$$m \ddot{x}_H + c \dot{x}_H = f_{xd} - f_x. \quad (4)$$

where  $x_H$  denotes the hand position controlled along the direction perpendicular to the object,  $f_x$  the force exerted at the hand, and  $m$  and  $c$  the mass and damper of impedance control respectively. In this control law,  $x_H$  is controlled so that  $f_x$  is regulated to converge to the desired force  $f_{xd}$ .

When using a humanoid robot platform, the robot should apply not only the necessary force to the hand for manipulation but also keep the balance of the whole body.

We adopt the method developed by Harada et al. known as balancing method [6]. The key idea is to control the CoM of the robot so that the “static balancing point” is on the center of the foot supporting polygon. The static balancing point is the point to which all the resistance force from both hands and gravity are applied, which is equivalent to ZMP when no dynamics motion is generated.

By introducing this control method the force of pivoting manipulation is generated as a resulting compensation of disturbance due to the contact with the object.

### B. Robot motion phase

After a sequence of manipulation, the object will be displaced to a farther position from the robot. Now the robot itself needs to move in the desired direction of object transportation. It is, therefore, preferable that robot keep the hands on the object to easily go on the manipulation. Here also, we introduce a control scheme of RMC to implement this motion. The hand position can be controlled based on an extended method of RMC developed by Neo et al. [13].

In this way, the robot can step towards the object with its both hands at the position keeping the contact, while the CoM is controlled always inside the convex hull of supporting area(s). Moreover, keeping the hand position on the object may help to maintain the equilibrium of the robot body.

## V. SIMULATION AND EXPERIMENT

To verify the proposed planning method, we perform simulation and experiment on humanoid platform HRP-2 [11]. HRP-2 has 30 degrees of freedom with 1.54[m] in height and 58[kg] in weight. Control software is implemented on humanoid robot simulator OpenHRP [10]. Thanks to the architecture of software OpenHRP, the developed simulation software has binary compatibility with the robot hardware.

### A. Stepping over obstacles

We use a box with depth of 50[mm] and height of 150[mm] as the obstacle. From our feasibility analysis, we know that this obstacle can be stepped over by HRP-2, since its height is less than the corresponding maximum height 242.1[mm].

The trajectories and orientation of the two feet in X-Z plane are shown in Fig. 6, where the shaded blue triangles indicate the foot configurations at four path control points, and the shaded red rectangle represents the obstacle. It can be seen that the feet surmount the obstacle without any collision.

Fig. 7 shows the components of the trajectories with time, from which the good smoothness of the curves can be observed. Fig. 8, Fig. 9 and Fig. 10 show some experimental snapshots of the robot in the three phases, respectively.

### B. Pivoting manipulation

1) *Experiment of manipulation phase:* We have conducted an experiment of pivoting manipulation. The information from the force sensors at the wrists is used for impedance control.

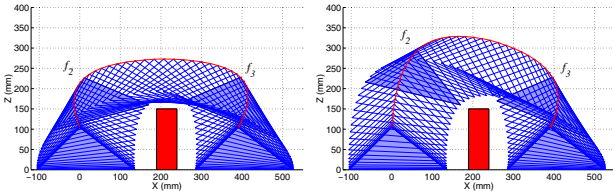


Fig. 6. Trajectories of front foot (in phase 1) and rear foot (in phase 3)

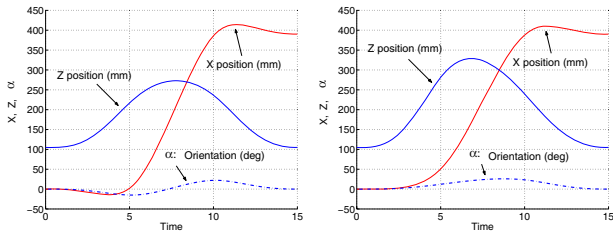


Fig. 7. Components of foot trajectories with time

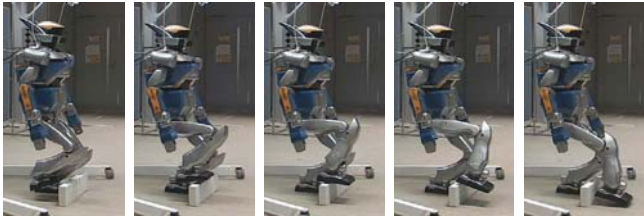


Fig. 8. Experiment of obstacle stepping-over (Phase 1)

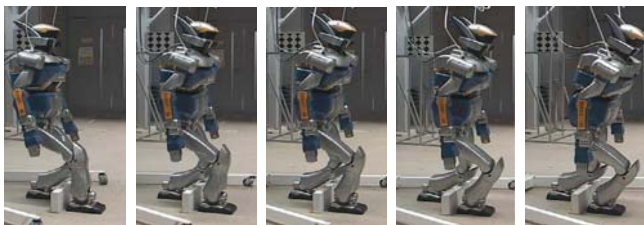


Fig. 9. Experiment of obstacle stepping-over (Phase 2)

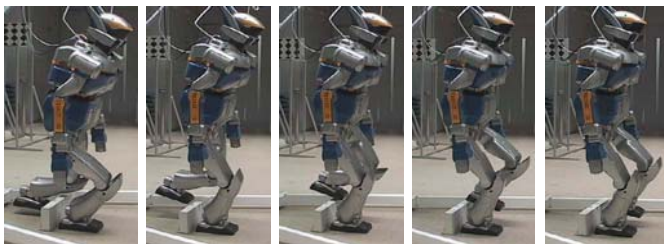


Fig. 10. Experiment of obstacle stepping-over (Phase 3)

Since the output of force sensor is somewhat noisy, we use an average value of the last 20 samplings measured every 5 [ms]. The width, depth, and height of the object are 350[mm], 200[mm], and 1200[mm] respectively. The mass is approximately 3[kg].

In the manipulation, two sequences including steps Fig. 4(a) ~ (c) are performed by changing the contacting vertex  $v$  from near-right to near-left. The rotation angle is  $-15[\text{deg}]$  in the first sequence and then  $15[\text{deg}]$  in the second. Other parameters of the pivoting sequence is selected such that the angle between  $a$  and the object side edge takes  $18.4[\text{deg}]$ ,  $z$  equals to the vertical axis, and inclination angles is  $5[\text{deg}]$ , respectively. Here parameter  $D$  is set to  $50[\text{mm}]$  to prevent the arms from going into singular configuration and losing stability by extending arm too much.

For the impedance control, we adopt  $m = 10[\text{kg}]$ ,  $c = 300[\text{N}\cdot\text{m}^{-1}\cdot\text{s}]$  and  $f_{xd} = 25[\text{N}]$  respectively. The internal force  $f_{xd}$  is determined for the robot to grasp firmly to prevent the object from slipping because of gravity. The height position of grasping is set to  $620[\text{mm}]$ .

Figure 11 shows snapshots of the experiments. As can be seen, the pivoting manipulation has been executed appropriately and the displacement in forward direction was around  $60[\text{mm}]$  as expected from simulation. In the experiments, the desired internal force has been maintained accurately enough, although the force decreased at the last stage of manipulation. The CoM position stayed in the supporting area, which shows the effectiveness of balance control.

This result demonstrates the effectiveness of the proposed manipulation method. Configuration and grasping position need to be investigated for more reliable manipulation in the future work.

2) *Simulation of robot motion phase:* The robot motion phase is simulated based on the proposed method. Figure 12 shows the sequence of stepping for forward motion. After the

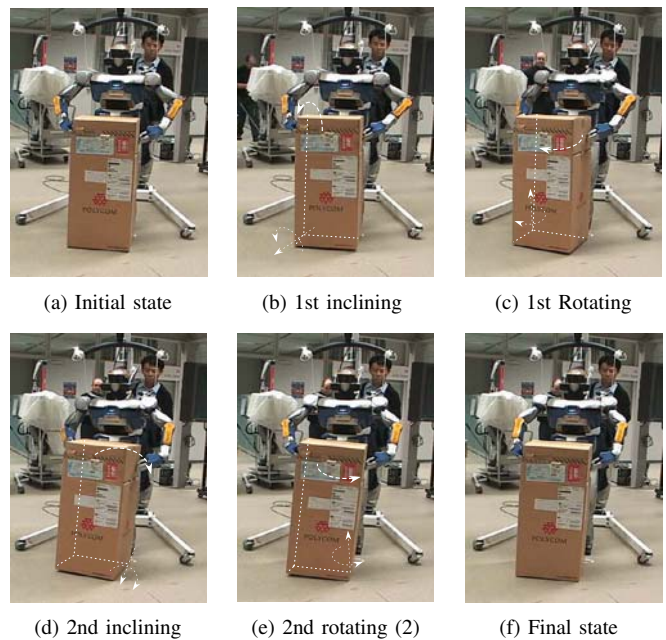


Fig. 11. Experiment of pivoting motion

manipulation, the robot steps forward by 50[mm] by moving its feet alternatively, by keeping the hand on the object using RMC to maintain the whole body balance. As shown in Fig. 12, first robot moves its CoM on the right foot and then moves the left foot forward. The same sequence is repeated for the right foot. The simulation shows that robot can effectively moves towards the desired direction of manipulation.

In the current development, only the position control and straightforward motion is implemented. This method will be extended to enable the robot to keep the desired grasping force by impedance control and to transport the object along arbitrary trajectories.

## VI. CONCLUSIONS

We have presented methods of motion planning for whole body tasks by a humanoid robot. As basic tasks, we have investigated the problems of stepping over obstacles and manipulating large objects.

For the obstacle stepping-over task, a novel algorithm was presented for motion planning of humanoid robots. Two basic requirements, namely, collision avoidance and robot balance, have been taken into account in planning for motion of the lower body and the upper body, respectively. Since the trajectories are determined based on our previous feasibility analysis and according to obstacle size, the method is adaptive to various obstacles, and therefore can be used in autonomous implementation of obstacle stepping-over of humanoid robots guided by vision. Simulation and experiment have verified the effectiveness of the proposed planning method.

For the manipulation task, a planning method has been developed for pivoting a large object, composed of manipulation and robot motion phases by a humanoid robot. After the object is moved towards the desired direction by grasping it by two arms, then robot makes steps in the same direction to continue the manipulation task. Impedance control was introduced to control the internal force, and resolved momentum control

was adopted for stepping motion keeping the contact of both hands with the object. The method will be improved to adapt to various object shapes and trajectory of transportation in pursuit of wide application in future developments. In future work, dynamic humanoid motion will need to be addressed for more efficient task execution for both cases.

We have demonstrated that the proposed planning method can be effectively performed by experiments and simulations.

## ACKNOWLEDGMENTS

We would like to express our sincere thankfulness to Dr. Shuji Kajita and Dr. Kensuke Harada of Humanoid Research Group, Intelligent Systems Research Institute, AIST, for their helpful advice on implementation of resolved momentum control and impedance control.

## REFERENCES

- [1] Y. Aiyama, M. Inaba, and H. Inoue. "Pivoting: A new method of grasplless manipulation of object by robot fingers," *Proc. of the IEEE/RSJ Int. Conf. on Intelligent Robots and Systems*, 136-143, 1993.
- [2] R. Bartels, J. Beatty, and B. Barsky. *An Introduction to Splines for Use in Computer Graphics and Geometric Modelling*. Morgan Kaufmann, 1998.
- [3] P. Channon, S. Hopkins, and D. Phan. Derivation of optimal walking motions for a biped walking robot, *Robotica*, 10(2):165-172, 1992.
- [4] Y. Guan, K. Yokoi, and K. Tanie. Feasibility: Can humanoid robots overcome given obstacles? *Proc. of IEEE Int. Conf. on Robotics and Automation*, 1066-1071, 2005.
- [5] H. Harada, S. Kajita, F. Kanehiro, K. Fujiwara, K. Kaneko, K. Yokoi, and H. Hirukawa. Real-Time Planning of Humanoid Robot's Gait for Force Controlled Manipulation, *Proc. of IEEE Int. Conf. on Robotics and Automation*, 616-622, 2004.
- [6] H. Harada, S. Kajita, H. Saito, M. Morisawa, F. Kanehiro, K. Fujiwara, K. Kaneko, and H. Hirukawa. A Humanoid robot carrying a heavy object, *Proc. of IEEE Int. Conf. on Robotics and Automation*, 2005, to appear.
- [7] Q. Huang, K. Yokoi, S. Kajita, K. Kaneko, H. Arai, N. Koyachi, and K. Tanie. Planning walking patterns for a biped robot, *IEEE Transactions on Robotics and Automation*, 17(3):280-288, 2001.
- [8] Y. Hwang, A. Konno and M. Uchiyama. Whole body cooperative tasks and static stability evaluations for a humanoid robot, *Proc. of IEEE/RSJ Int. Conf. on Intelligent Robots and Systems*, 1901-1906, 2003.
- [9] S. Kajita, F. Kanehiro, K. Kaneko, K. Fujiwara, K. Harada, K. Yokoi, and H. Hirukawa. Resolved momentum control: Humanoid motion planning based on the linear and angular momentum, *Proc. of IEEE/RSJ Int. Conf. on Intelligent Robots and Systems*, 1644-1650, 2003.
- [10] F. Kanehiro, N. Miyata, S. Kajita, K. Fujiwara, H. Hirukawa, Y. Nakamura, K. Yamane, I. Kohara, Y. Kawamura and Y. Sankai: Virtual humanoid robot platform to develop controllers of real humanoid robots without porting, *Proc. of IEEE/RSJ Int. Conf. on Intelligent Robots and Systems*, 1093 - 1099, 2001.
- [11] K. Kaneko, F. Kanehiro, S. Kajita, H. Hirukawa, T. Kawasaki, M. Hirata, K. Akachi and T. Isozumi. The Humanoid Robot HRP-2, *Proc. of IEEE Int. Conf. on Robotics and Automation*, 1083-1090, 2004.
- [12] J. Kuffner, S. Kagami, K. Nishiwaki, M. Inaba, and H. Inoue. Dynamically-stable motion planning for humanoid robots. *The Journal of Autonomous Robots*, 12(1):105-118, 2002.
- [13] N. E. Sian, K. Yokoi, S. Kajita, K. Tanie. Whole Body Teleoperation of a Humanoid Robot Integrating Operator's Intention and Robot's Autonomy - An Experimental Verification -, *Proc. of IEEE/RSJ Int. Conf. on Intelligent Robots and Systems*, 1651-1656, 2003.
- [14] L. Roussel, C. Canudas de wit, and A. Goswami. Generation of energy optimal complete gait cycles for biped robots. In *Proc. of IEEE Int. Conf. on Robotics and Automation*, 2036-2041, 1998.
- [15] T. Takubo, K. Inoue, K. Sakata, Y. Mae, and T. Arai. Mobile Manipulation of Humanoid Robots - Control Method for CoM Position with External Force -, *Proc. of IEEE/RSJ Int. Conf. on Intelligent Robots and Systems*, 1180-1185, 2004.
- [16] E. Yoshida, V. Hugel, and P. Blazevic: Pivoting Manipulation of a Large Object: A Study of Application using Humanoid Platform, *IEEE Int. Conf. on Robotics and Automation*, 1052-1057, 2005.

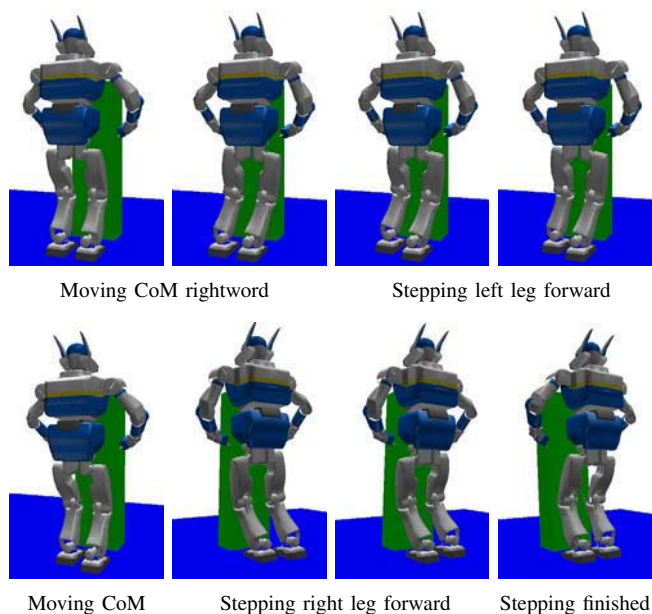


Fig. 12. Stepping forward keeping the hands on the object